Clean Technologies and Recycling

Clean Technologies and Recycling, 5 (1): 22–43.
DOI: 10.3934/ctr.2025002
Received: 23 August 2023
Revised: 27 January 2025
Accepted: 18 February 2025
Published: 10 March 2025

http://www.aimspress.com/journal/ctr

Research article

Leaching kinetics of ZN^{2+} and SO_4^{2-} from tire pyrolytic char (TPC) using the shrinking core model

Lucky Malise[1], Hilary Rutto[2,*] Tumisang Seodigeng[1] and Linda Sibali[3]

[1] Clean technology and applied materials research group, Department of Chemical and Metallurgical Engineering, Vaal University of Technology, Private Bag X021, South Africa
[2] Department of Chemical Engineering, Durban University of Technology, Private Box 1334, Durban, 4000, South Africa
[3] Department of Environmental Sciences, College of Agriculture and Environmental Sciences, UNISA, Florida, 1709, South Africa

*** Correspondence:** Email: hilary.rutto@gmail.com.

Abstract: Tire pyrolytic char has the potential to be used as a raw material/product in different applications. The only problem associated with the tire pyrolytic char is the presence of some impurities, which limits its potential for use as carbon black and as a precursor to producing activated carbon. Tire pyrolytic char contains high concentrations of Zn^{2+} and S, which are used as ingredients while manufacturing tires. Our main aim of this study was to perform leaching studies to remove of Zn^{2+} and SO_4^{2-} from the tire pyrolytic char using a solution of H_2O_2 as a solvent and to perform kinetic studies further using the shrinking core model to determine the rate-limiting step for the leaching of Zn^{2+} and SO_4^{2-}. Process variables such as stirring speed (rpm), solvent concentration (ppm), temperature (°C), and solid-to-liquid ratio (g/100 ml) were investigated. It was found that the leaching rate of Zn^{2+} and SO_4^{2-} from the pyrolytic tire char increased with an increase in all the process variables except for the solid to liquid ratio, which had an opposite effect on the leaching rate. Fourier Transform Infrared Spectra (FTIR) analysis, SEM-EDS, and Xray diffraction (XRD) analysis were used to characterize the pyrolytic tire char before and after the leaching experiments. FTIR showed that sulfur-containing functional groups disappeared after leaching with a solution of H_2O_2. SEM-EDS also showed a reduction in both Zn and S presence from the pyrolytic tire char after the leaching. XRD results showed that the raw tire pyrolytic char contained diffraction peaks associated with ZnO and ZnS, which disappeared after exposure to leaching. The kinetic parameters obtained showed that the rate-limiting step for the leaching of Zn^{2+} and SO_4^{2-} from tire pyrolytic char was diffusion through the

product layer. The regression coefficients obtained for diffusion through the product layer for both Zn^{2+} and SO_4^{2-} were closer to 1 than values obtained for the chemical reaction between the fluid reactant with the solid at the surface of the solid particle. This was further confirmed by the apparent activation energies obtained for the leaching of Zn^{2+} and SO_4^{2-} -11 kJ.mol^{-1} and 36 kJ.mol^{-1}, respectively. Semi-empirical models for the leaching of Zn^{2+} and SO_4^{2-} were developed to describe the leaching process.

Keywords: tire pyrolytic char; leaching; shrinking core model; semi-empirical model

1. Introduction

The global demand for mobile auto tires has been growing throughout recent years due to the increased use of automobiles. It was predicted that a total of 2.5 billion units of tires would be in demand by the year 2022 [1], and another study by [3,4] revealed that the global market for tires will reach 2.67 billion units by 2027. Consequently, this will add to the significant number of waste tires that are present. Some environmental problems are associated with the increased generation of waste tires stemming from the difficulty in disposing of them in an environmentally friendly manner.

The manufacture of waste tires is a complex process that uses several ingredients to produce tires with specific properties. The primary ingredients in the manufacture of tires are natural and synthetic rubber. As a result, the tire industry is the largest consumer of natural and synthetic rubber. Natural rubber in tires is found in cis-1,4-polyisoprene, while synthetic rubber is found in Stirene Butadiene Rubber, Butyl Rubber, and Isobutylene Isopropylene Rubber [2]. In the manufacture of tires, natural rubber and different types of synthetic rubber are vulcanized together in the presence of sulfur to form a composite with specific properties required for the tire [2]. Natural and synthetic rubber in tires are found in the tire treads, and the sidewalls of the tires and the composition of these rubbers on the tires differ depending on the type of tire being manufactured [3]. The second most important ingredient in the manufacture of tires is carbon black, amounting to about 20–30 wt % of the tire. Carbon black is a reinforcement filler in tires to improve tire tensile and tear strength, abrasion resistance, and other mechanical properties [4].

Other essential ingredients used to manufacture tires include metals, textiles, vulcanization agents, and additives. Metals such as steel and steel alloys are used in the tire beads and belts in different proportions depending on the type of the tire. These beads are in tires to connect the tire and the wheel rim, while the beads filler serves as a transition between the beads wire and the inner liner [2]. Textiles such as polyester nylon and natural rayon are used to manufacture tires as a substitute for metals in lighter tires [5]. Vulcanization agents and additives such as sulfur groups, zinc oxide, antioxidants, and antiozonants are used in the vulcanization process to manufacture tires. Vulcanization is a process utilized to convert natural rubber and synthetic rubber into a crosslinked structure of rubber [6]. Vulcanization is an irreversible process responsible for tire properties such as elasticity, higher deformation resistance, and biodegradable resistance.

These properties of tires are the primary reason it is difficult to dispose of waste tires in an environmentally friendly way. Tires are considered non-biodegradable, and as a result, they do not decompose, and they can persist in the environment for many years if they are not properly disposed of. On many occasions, waste tires are stockpiled or landfilled, and these disposal methods are not

environmentally friendly; instead, they lead to the loss of value from waste tires and pose some environmental and health issues in society. Waste tire management is governed by laws and regulations that seek to ensure the environmentally responsible disposal of waste tires in South Africa. The National Environmental Management Act, 2008 (Act No. 59 of 2008) provides a framework for waste management, including the management of waste tires in South Africa. The act emphasizes the need for waste tire minimization, the importance of waste tire recycling, and the need for and importance of responsible disposal of waste tires. The Act mandated that waste tires must be managed in an environmentally sound manner, which included requirements for the proper storage, collection, and processing to prevent environmental pollution and health hazards. It also required tire producers and importers to develop and implement waste tire management plans, ensuring that they take responsibility for the entire lifecycle of their products. The Act established licensing requirements for facilities handling tire waste and set strict penalties for non-compliance, reinforcing the need for adherence to high environmental standards. The 2017 amendments to the NEMA Waste Act further increased the stringency in managing waste tires by introducing the concept of Extended Producer Responsibility (EPR). This required producers to be accountable for the end-of-life management of tires, encouraging more proactive approaches to recycling and waste reduction. The amendments also included more rigorous criteria for waste management licensing, enhanced compliance and enforcement powers for environmental authorities, and stricter penalties for violations. Additionally, the amendments mandated the establishment of national norms and standards for waste management activities and set specific targets for waste minimization and recycling. These changes aimed to improve the overall efficiency and effectiveness of tire waste management, ensuring greater environmental protection and sustainability.

Pyrolysis is a thermal treatment process that has been viewed as a promising technique for recovering energy from waste tires due to their high calorific value and high carbon content. The process can reduce the weight percent of waste tires by up to 90 % of their original weight and produce products such as waste tire pyrolytic oil, char, and gas. Through further processing, the pyrolytic oil can be upgraded and used in boilers and as feedstock in petroleum refineries [7,8]. The pyrolytic gas obtained from the pyrolysis of waste tires is said to have a high calorific value. It finds its use as fuel to supplement the energy requirements for the pyrolysis process [9]. On the other hand, the pyrolytic char has been gaining attention due to its properties. The solid product from the pyrolysis of waste tires accounts for up to 30–40 % of the waste tire weight. Through further processing, the char can be used as carbon black to manufacture waste tires as a reinforcement filler [10]. The pyrolytic char has desirable physical properties and can also be used as a precursor in producing activated carbon with high internal surface area and good adsorptive characteristics. The problem associated with waste tire pyrolytic char for use as a precursor of activated carbon is concentrations of Zinc and sulfur, which are considered undesirable for use as a precursor. Sulfur and Zinc are used in the production of rubber tires during the vulcanization process to introduce crosslinks elastomers' polymer matrix [11]. The vulcanization process using sulfur and zinc oxide increases the hardness, tensile strength, abrasion resistance, and rebound. It improves other properties of the rubber tire, which is a critical step in producing rubber tires [12].

To combat this issue, research has been done on the leaching of Zinc and sulfur from the char before the activation step to produce activated carbon. It has been reported that process variables such as solid/liquid ratio, solvent concentration, agitation speed, pH, leaching time, temperature, and particle size of the solid sample influence the leaching rate [13,14]. Yamaguchi et al. [14] reported that

leaching of the waste tire pyrolysis char with hydrochloric acid and activation of the resulting char with steam at 925 °C for 520 min resulted in the production of waste tire activated carbon with a BET surface area of 1022 m^2/g. The effects of molten salt thermal treatment on the properties improvement of waste tire pyrolytic char were investigated by Zou et al. [15]. According to their findings, molten salt thermal treatment can effectively remove impurities from various pyrolytic chars, with the best reaction conditions being 400 °C, 2 hours of reaction time, and a molten salt/char ratio of 10:1. Furthermore, the pyrolytic char's graphite carbon content was increased from 24.41% to 70.90%, and the hydroxyl content on the pyrolytic char surface significantly increased. Jiang et al. [16] investigated the recovery of high pure pyrolytic carbon black from waste tires using dual-acid treatment. They discovered that their leaching process could effectively remove more than 80% of ash and 70% of sulfur at 400 °C, with char recovery rates ranging from 71% to 83%.

Furthermore, molten salts demonstrated good activity in converting char-containing inorganic sulfides and SH radicals into salts-soluble Na_2S. Similarly, silicon and zinc tended to be converted into soluble silicate and zincate, which had good solubility in the used molten salt. It was also reported that the amount of sulfur and Zinc in the char decreased because of leaching with hydrochloric acid. Other studies observed similar behavior concerning the decrease in the zinc and sulfur content and an increase in the BET surface area obtained after activation with steam [17]. The homogeneous model, uniform pore model, grain model, and shrinking core model (SCM) are a few kinetic models that have been put out in the literature to describe the kinetics of dissolution of solid material [18]. Since it is the most straightforward description for most industrial solid-fluid processes, the authors developed the shrinking core model to describe waste tire pyrolytic char dissolving kinetics. Here, we use the SCM to forecast how zinc and sulfate ions will dissolve over time from waste pyrolytic char made from used tires. As a result, the mathematical model can precisely forecast zinc and sulfate ions leaching from pyrolyzed waste tire char.

The kinetics of processes in a solid-state material are described using the shrinking core model (SCM), a frequently used concept in chemical engineering. According to this hypothesis, a solid particle comprises numerous layers, the outermost layer reacting with the gas or liquid around it. Shrinkage of the particle's layers occurs as the reaction develops, giving rise to the term "shrinking core." To explain the kinetics of reactions and the rate-limiting step, the SCM is frequently employed in industrial reaction applications. In desulfurization and hydrometallurgical reactions, SCM is used to study the kinetics of heterogeneous reactions, which involve a reactant gas or liquid passing over a solid catalyst [19–22]. The SCM can help determine the rate-limiting step in the reaction, optimizing the process and performance. Li et al. [35] studied zinc leaching recovery and mechanisms from end-of-life tires. The results obtained from the study revealed that 98% of ZnO particles can be removed from waste tires and that the leaching process was controlled by diffusion. Although there are researchers focusing on the leaching process and kinetics of Zn from waste tires, there is little research on the leaching of Zn^{2+} and SO_4^{2-} from waste tire pyrolytic char. We aim to investigate how the different process variables affect the leaching of Zinc (Zn^{2+}) and Sulfates (SO_4^{2-}) from waste tire pyrolytic char (TPC) before activating the pyrolytic char to produce carbon black. We also focus on the leaching kinetics using the shrinking core model to determine the rate-limiting step for the leaching process, which is not well documented in the literature.

2. Materials and Methods

2.1. Materials

The primary material for this study was tire pyrolytic char (TPC) obtained from a local supplier. The waste tire pyrolytic char was produced through the pyrolysis of waste tire rubber in a fixed bed reactor operating at a temperature of 700 ºC for 2 hours under a nitrogen atmosphere as per the supplier's standard pyrolysis conditions. Hydrogen Peroxide (H_2O_2) was used as the solvent for the leaching experiments, and it was obtained from Rochelle Chemicals and Lab Equipment. H_2O_2 was used as a solvent in this study because it is a weak acid with high oxidation potential. Other chemical reagents such as Hydrochloric Acid and Sodium Hydroxide were used to adjust the pH value of the solutions before the leaching experiments. These reagents were obtained from Sigma Aldrich (Pty).

2.2. Methods

A total of 100g of tire pyrolysis char (TPC) was washed thoroughly with distilled water to eliminate impurities. The washed sample was then placed in a drying oven operating at 100 °C for 24 hours to remove moisture from the sample. The dry sample was then sieved to a particle size of 100 µm and stored in a sealed container before further use.

2.3. Characterization techniques

2.3.1. Fourier Transform Infrared Radiation (FTIR) analysis

FTIR analysis was performed on the tire pyrolysis char (TPC) sample to determine the surface functional groups present on the raw sample before the leaching experiments and on the sample after different conditions of the leaching experiments. A Perkin Elmer spectrum (400FT-IR/FT-NIR) was used for this purpose, and the samples were scanned and recorded in the range of 400 – 4500 cm^{-1}. The Diffuse Reflectance Infrared Fourier Transform adapter measuring technique was used as described by [32] since the technique allows for the substance being measured to be analyzed in powder form and does not require the formation of a solid tablet prior to analysis.

2.3.2. Scanning Electron Microscopy (SEM) analysis

A Phillips XL 30S scanning electron microscope was used to determine the morphology of the tire pyrolysis char (TPC) sample. This was done by scattering the samples on an adhesive carbon plate and sputter coating the sample with a thin layer of gold before conducting the SEM analysis. After leaching experiments, the analysis was done for the raw (TPC) and the (TPC) samples.

2.3.3. X-ray Diffraction (XRD) analysis

XRD analysis was performed on the tire pyrolysis char (TPC) sample to determine its phase analysis before and after the leaching experiments. The analysis was performed using a PANalytical Empyrean diffractometer with a pixel detector and fixed slits with Fe-filtered CO-Kα radiation. An X'Pert High score plus software was used to identify the phases, and the relative phase amounts (weight %) were estimated using the Rietveld method.

2.3.4. Leaching experiments

Leaching experiments of Zn^{2+} and SO^{4-} from pyrolytic tire char (TPC) were carried out in batch processes using 200ml sealed Erlenmeyer flasks, a magnetic heating plate with a stirrer, and a thermometer. Process variables such as temperature, solvent (H_2O_2) concentration, solid-liquid ratio, stirring speed, and leaching time were investigated on how they influence the leaching rate. Data from these experiments were also applied to the shrinking core model to determine the rate-limiting step for the leaching process. Table 1 illustrates the experimental design for the process variables varied and the experimental conditions used for the leaching experiments.

Table 1. Experimental design showing the experimental conditions for the leaching experiments.

Process variable	**Experimental condition**			
Temperature (°C)	30	45*	60	75
Stirring Speed (rpm)	50	100	150*	200
Solvent concentration (M)	0.5	1	1.5*	2
Solid/Liquid ratio (g/100 ml)	0.5	1*	1,5	2

The values with a (*) superscript show that each process variable was held constant.

The concentrations of Zn^{2+} and SO_4^{2-} in solution were measured using Atomic Absorption Spectrometer (AAS) and Infrared Chromatography. Equation 1 below was used to determine the value of the leaching rate (X):

$$X = \frac{Zn^{2+} or\ SO_4^{2-}\ in\ solution\ after\ leaching}{Zn^{2+} or\ SO_4^{2-}\ in\ the\ original\ waste\ tyre\ pyrolytic\ char\ sample} \quad (1)$$

where X is the leaching rate (ppm/ppm), Zn^{2+} or SO_4^{2-} in solution after leaching are the concentration of Zn^{2+} or SO_4^{2-} that remain in solution after leaching experiments (ppm), and Zn^{2+} or SO_4^{2-} in the original waste tire pyrolytic char sample are the initial concentrations of Zn^{2+} or SO_4^{2-} in the solid char sample before the leaching experiments (ppm).

3. Results and discussion

3.1. Characterization of TPC

3.1.1. Fourier Transform Infrared Radiation analysis

Fourier Transform Infrared Radiation analysis was performed on the raw tire pyrolytic char (TPC) before leaching experiments with hydrogen peroxide and after 2 hours. This was to determine the surface functional groups present in the raw char and the char after leaching. The FTIR spectrum was recorded between the range of 400 and 4500 cm^{-1} wavenumbers for the samples analyzed. The conditions for FTIR analysis after leaching experiments at the solid-liquid ratio, stirring speed, temperature, solvent concentration, and contact time of 1 g/100 ml, 150 rpm, 45 ºC, 1.5 M, and 30 min, respectively. Figure 1 depicts the FTIR spectrums obtained from the analysis. The raw tire pyrolytic char (TPC) sample shows sulfur-containing functional groups observed at bands 2600, 2150, 1400, and 1350 cm^{-1}. After leaching for 2 hours, the presence of sulfur-containing functional groups either disappeared or diminished slightly due to the leaching effect of hydrogen peroxide on the

pyrolytic tire char. A similar observation on the removal of sulfur and metallic elements from the pyrolytic tire char through leaching with acids, hydrogen peroxide, and nitric acid has been reported by Seng-eiad and Jitkarnka [23]. Similar observations were made by [33] as a band representing sulfoxide experienced at 1030 cm^{-1}.

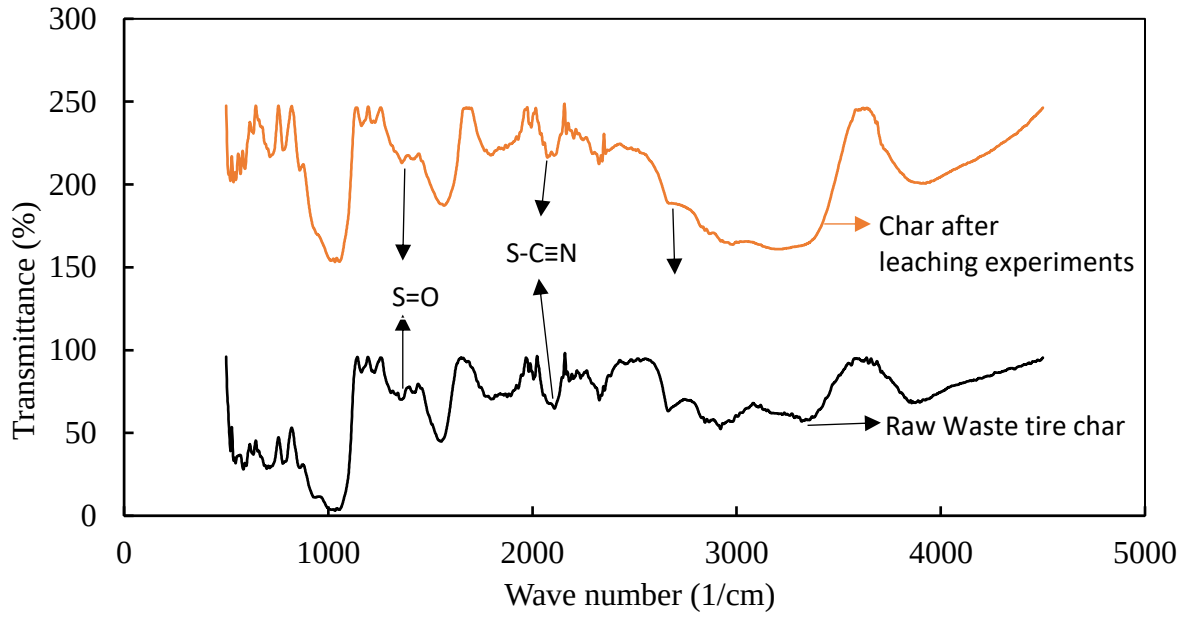

Figure 1. Fourier Transform Infrared Radiation spectra for the tire pyrolysis char before and after leaching with hydrogen peroxide

3.1.2. Scanning Electron Microscopy (SEM) analysis

Table 2 represents the EDS elemental analysis of the tire pyrolytic char samples before and after leaching with hydrogen peroxide. The EDS elemental analysis results in Table 2 are averages of three samples observed during the analysis. The experimental leaching conditions for solid-liquid ratio, stirring speed, temperature, solvent concentration, and contact time were 1 g/100 ml, 150 rpm, 45 ºC, 1.5 M, and 45 min, respectively. The table shows that the sulfur and zinc contents were 1.79 and 3.48 weight %, respectively, in the raw tire pyrolytic char. After subjecting the raw tire pyrolytic char to leaching experiments with 1M hydrogen peroxide for 15 min, it can be observed that the sulfur and zinc content in the tire pyrolytic char reduced to 1.22 and 2.26 weight %, respectively. The same behavior was observed at other leaching time intervals. The optimum leaching contact time can be observed to be 1 hour 30 min, at which the sulfur and zinc content was reduced to 0.47 and 1.21 weight %, respectively. Similar behavior was reported by Seng-eiad and Jitkarnka [23] in their study. It was stated that leaching the pyrolytic tire char with nitric acid, hydrogen peroxide, and hydrochloric acid results in the demineralization of the pyrolytic tire char.

Table 2. EDS elemental analysis of the waste tire char before and after leaching at different time intervals.

Sample ID	C (wt.%)	O (wt.%)	Al (wt.%)	Si (wt.%)	S (wt.%)	K (wt.%)	Zn (wt.%)	Total (wt.%)
Raw Char	81.58	10.83	0.19	1.99	1.79	0.13	3.48	100
15 min	84.6	9.77	0.19	1.97	1.22	0	2.26	100
30 min	85.39	10.11	0.16	1.91	0.94	0	1.69	100
1 hour	85.22	9.75	0.21	2.18	1.02	0	1.62	100
1hr 30 min	82.33	14.45	0	1.54	0.47	0	1.21	100
2 hours	85.13	10.17	0.19	1.75	0.8	0	1.96	100

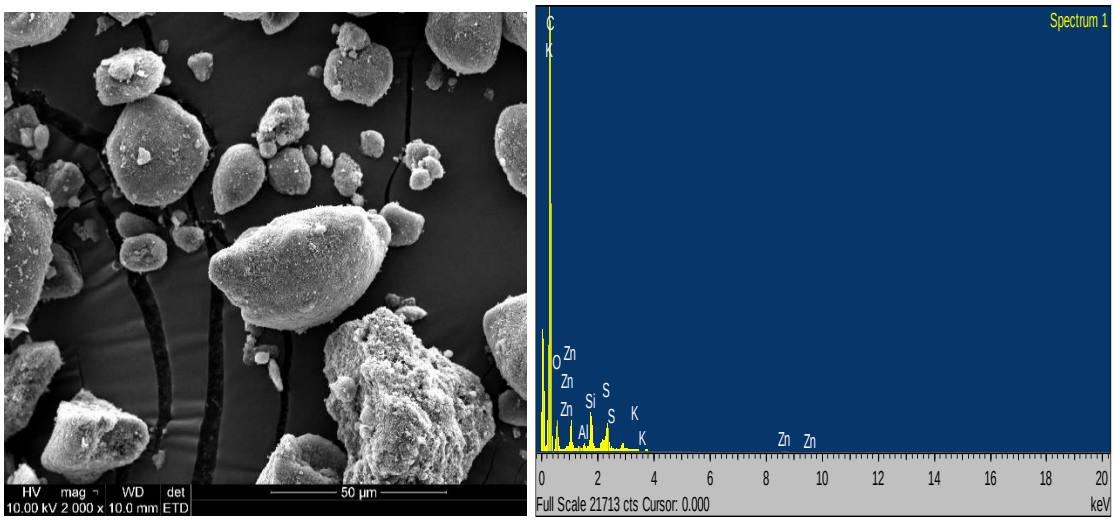

Figure 2. Scanning electron micrograph of raw tire pyrolytic char and identifying minerals by EDS.

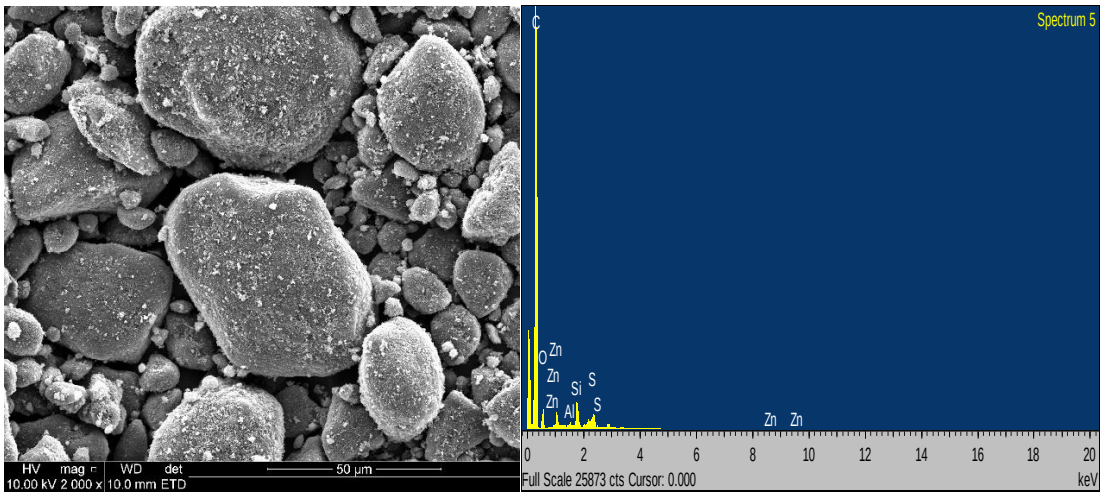

Figure 3. Scanning electron micrograph of tire pyrolytic char after 15 min leaching with hydrogen peroxide and identifying minerals by EDS.

Figures 2–5 show the SEM/EDS profiles for the pyrolytic tire char before and after leaching with hydrogen peroxide at different intervals. The SEM images of the samples before and after leaching experiments do not show much difference in their morphologies. This agrees with a study by Manoj [24], who reported a similar observation. The SEM images show that the morphologies of the samples were quite similar. However, the EDS profiles reveal that the sulfur and inorganic matter content was significantly higher in the waste tire char than in the samples analyzed after the leaching experiments. This is attributable to the leaching effect of the hydrogen peroxide on the pyrolytic tire char, which removed minerals from the surfaces of the waste tire chars.

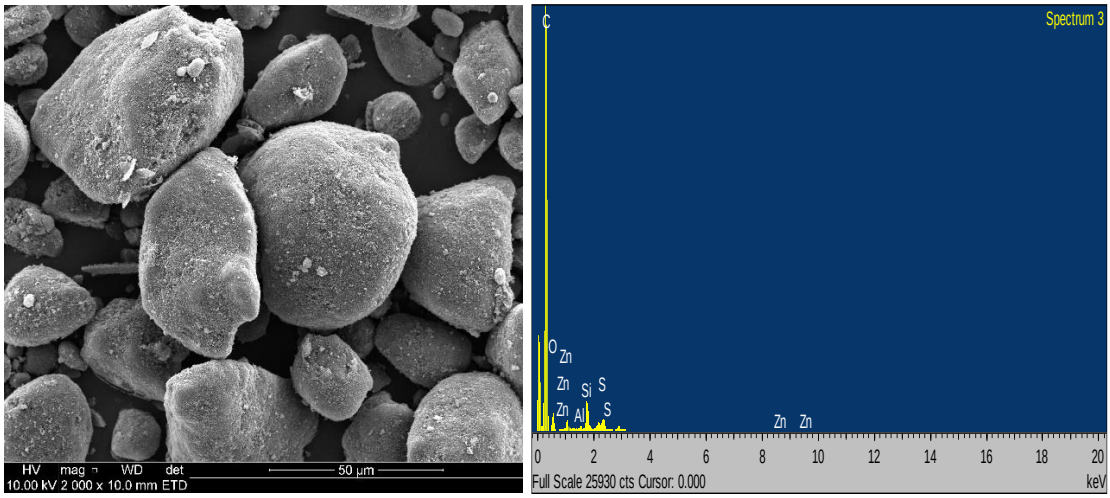

Figure 4. Scanning electron micrograph of tire pyrolytic char after 1 hr leaching with hydrogen peroxide and identifying minerals by EDS.

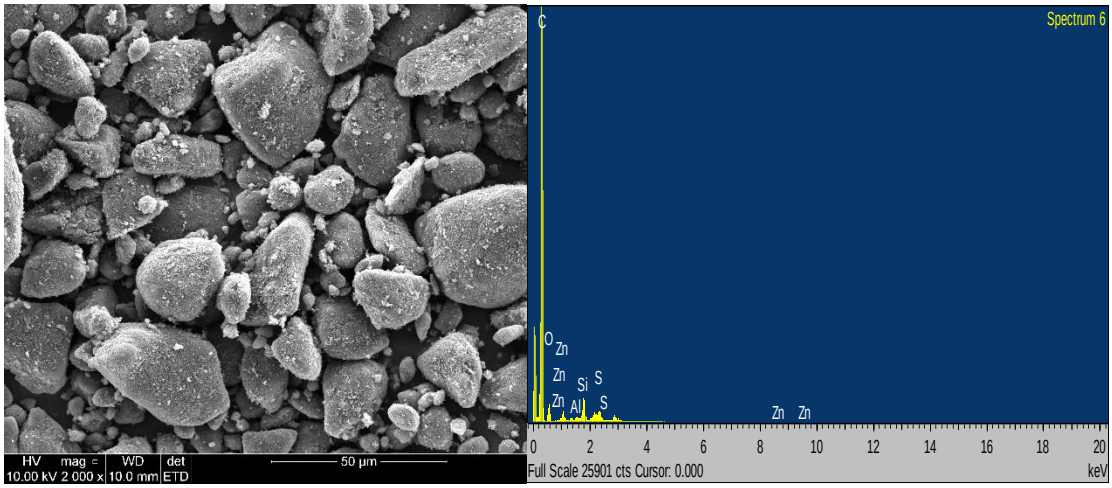

Figure 5. Scanning electron micrograph of tire pyrolytic char after 2 hr leaching with hydrogen peroxide and identifying minerals by EDS.

3.1.3. X-ray Diffraction (XRD) analysis

Figure 6 shows the XRD patterns for the raw tire pyrolytic char before and after leaching with hydrogen peroxide at different time intervals. The raw tire pyrolytic char shows diffraction peaks at

2θ = 29°, 34°, 55°, and 66°. These diffraction peaks are associated with the presence of ZnO and ZnS. After leaching experiments for 15 min, 1 hr, and 2 hr, the diffraction peaks associated with ZnO and ZnS disappeared, which can be attributed to the leaching effect of H_2O_2 causing Zn^{2+} and SO_4^{2-} to dissolve in solution from the pyrolytic tire char. A study by [36] evaluated the crystallinity of tire chars prepared under various conditions using microwave pyrolysis. Their study reported that tire pyrolytic char prepared through microwave pyrolysis contains similar diffraction peaks as the raw tire pyrolytic char from this study prior to leaching experiments. This nature of crystallinity was attributed to the presence of Zincite (ZnO) and Wurtzite (α ZnS). The study further reported that reference peaks associated with Zincite (ZnO) at 2θ = 31,85, 34,55, 36,36, 47,70, 56,75, 63,09, 68,17 and those associated with wurtzite (α ZnS) at 2θ = 26,81, 28,41, 30,42, 39,47, 47,36, 51,58, 56,16, and 57,33.

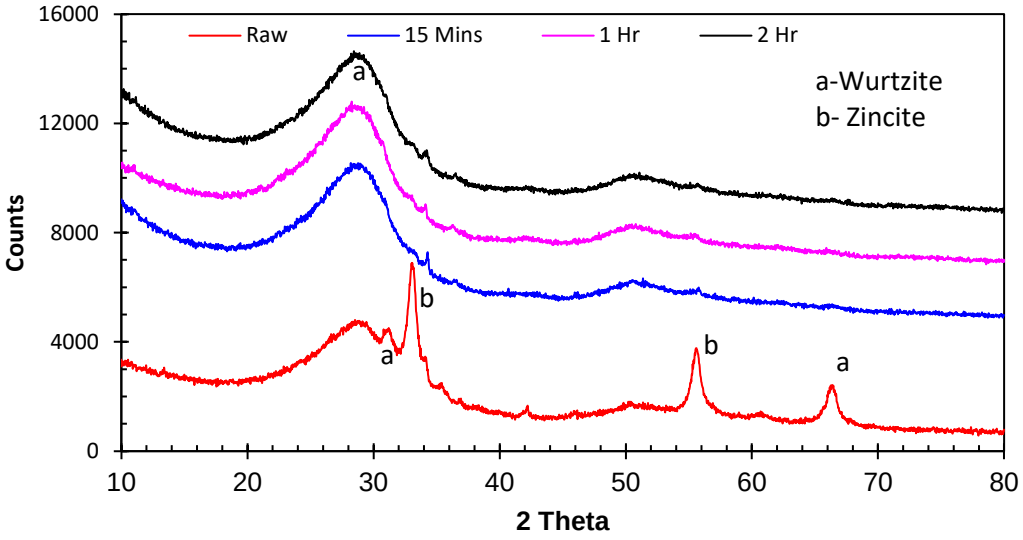

Figure 6. XRD patterns for the raw tire pyrolytic char and after leaching with hydrogen peroxide at different time intervals.

3.2. Effect of process variables on the leaching of Zn^{2+} and SO_4^{2-} ions from tire pyrolytic char

Figure 7A shows the plot of removal efficiency with time at different stirring speeds for the leaching of Zn^{2+} from tire pyrolytic char. It can be observed from the figure that the removal of Zn^{2+} increases exponentially until a point of equilibrium is achieved after 60 min, where there is no more significant impact on the leaching rate with the reaction time. An increase in the stirring speed from 0 rpm to 200 rpm results in a corresponding increase in the leaching rate of the ions from the pyrolytic tire char. This behavior can be attributed to effective contact between the tire pyrolytic char and hydrogen peroxide solution used as a solvent. This was similarly observed in the leaching of SO_4^{2-} from the pyrolytic tire char, as shown in Figure 8A; however, the equilibrium was achieved after a reaction time of 90 min.

3.2.1. Effect of temperature on the leaching of Zn^{2+} and SO_4^{2-} from tire pyrolytic char

The effect of temperature on the leaching of Zn^{2+} and SO_4^{2-} from pyrolytic tire char was investigated in the temperature range of 30 – 75 °C. Figure 7B shows that the temperature significantly

impacts the leaching rate for the Zn^{2+} ions. The conversion of Zn^{2+} into solution increased with an increase in the temperature from 30 to 60 °C and remained constant. There was a rapid increase in the leaching rate at shorter contact times and gradually decreased at longer contact times. A similar observation was made for the leaching of SO_4^{2-} as shown in Figure 8B. The increase in the leaching rate of both Zn^{2+} and SO_4^{2-} can be attributed to the decrease in the solvent's viscosity, which causes the liquid's diffusion coefficient to increase at higher temperatures. This results in more H^+ ions penetrating the inner core of the pyrolytic tire char and facilitating the decomposition of the Zn^{2+} and SO_4^{2-} ions into the solution [25].

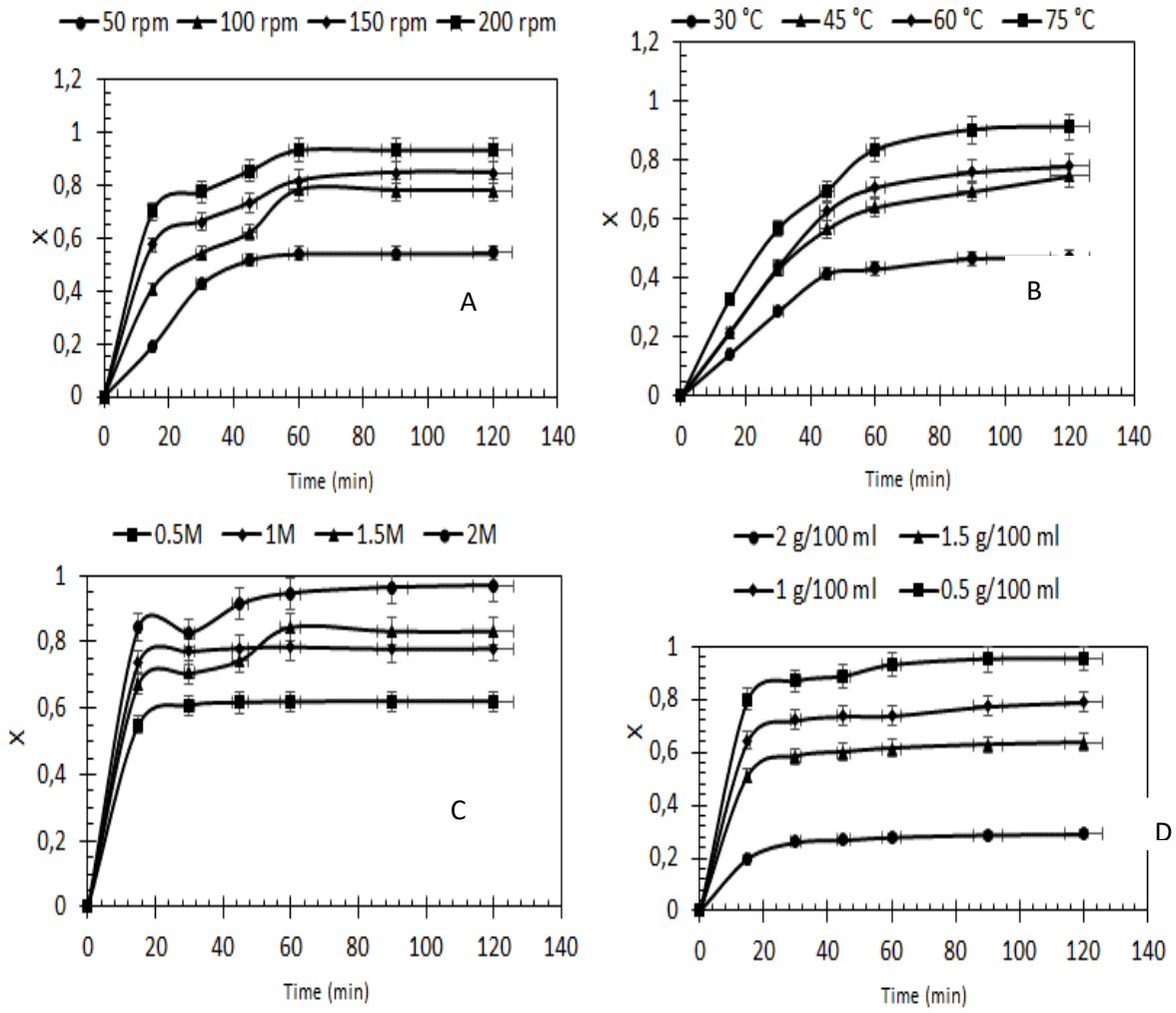

Figure 7. Conversion X (ppm/ppm) against time (min) on the effect of stirring Speed (A), Temperature (B), Concentration (C), and solid-to-liquid ratio (D) on the leaching of Zn^{2+}ions from tire pyrolytic char.

3.2.2. Effect of solvent concentration on the leaching of $Zn^{2+}$and SO_4^{2-} from tire pyrolytic char

The effect of solvent concentration on the leaching of Zn^{2+} is illustrated in Figure 7C. The figure shows that the leaching of the Zn^{2+} ions increases with the increasing concentration of hydrogen peroxide solvent. Figure 8C depicts the effect of the solvent concentration on the leaching of SO_4^{2-} which shows that an increase in the solvent concentration results in an increase in the removal of SO_4^{2-}

from the pyrolytic tire char. The maximum removal percentage for Zn^{2+} and SO_4^{2-} achieved from varying the solvent concentration was 95% and 70 %, respectively, at a solvent concentration of 2 M. A similar observation was made by [37] in their study focused on the leaching of rare earth metals from apatite ore. This behavior was said to be due to an insufficient amount of solvent at low concentrations for the liberation of heavy metals from the apatite.

3.2.3. Effect of solid/liquid ratio on the leaching of Zn^{2+} and SO_4^{2-} from tire pyrolytic char

Figures 7D and 8D depict the effect of solid/liquid ratio on the leaching of Zn^{2+} and SO_4^{2-}, respectively, using an H_2O_2 solvent. Both figures show that an increase in the solid/liquid ratio decreases the leaching rate. This behavior occurs because at low solid/liquid ratios, the concentrations of Zn^{2+} and SO_4^{2-} are low on the solid sample and result in high leaching rates. At high solid/liquid ratios, the concentrations of Zn^{2+} and SO_4^{2-} are high on the solid sample, and lower leaching rates are achieved compared to a lower solid-liquid ratio. A study by [38] reported that generally using a higher amount of lixiviant leads to increased leaching rates which is in agreement with the findings of this study.

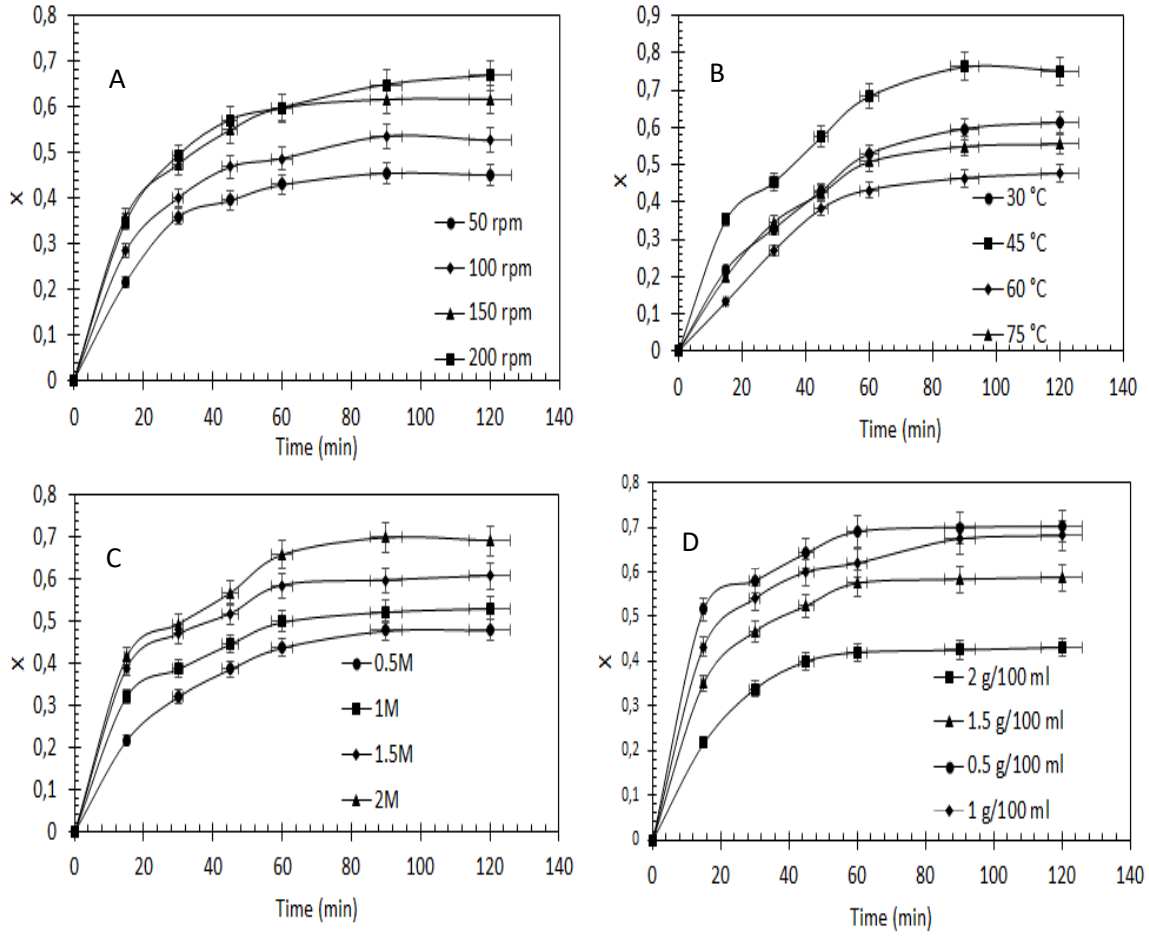

Figure 8. Conversion X (ppm/ppm) against time (min) on the effect of stirring Speed (A), Temperature (B), Concentration (C), and solid-to-liquid ratio (D) on the leaching of SO_4^{2-} ions from tire pyrolytic char.

3.3. Leaching kinetics of Zn^{2+} and SO_4^{2-} from tire pyrolytic char using the shrinking core model

Heterogeneous reaction systems (fluid-solid systems) are most described by the unreacted shrinking core model [18]. Using the shrinking core model, the reaction rate can be controlled by either one of the following three steps:

a. Diffusion through the liquid film layer.
b. Diffusion through the product layer.
c. A chemical reaction between the fluid reactant with the solid at the surface of the solid particle.

The rate-controlling step is considered the slowest of the three steps [26]. Diffusion through the liquid film layer can be avoided in this study as the rate-limiting step since the reacting fluid is in liquid form and does not restrict the reactant's transportation to the particle's surface [27]. The diffusion through the product layer and chemical reaction between the fluid reactant with the solid at the surface of the solid particle can be represented as follows in equations (2) and (3), respectively [18,31]:

$$1 + 2(1 - X) - 3(1 - X)^{2/3} = \frac{6bD_eC_A}{P_BR_0^2}t = K_dt \quad (2)$$

where X is the leaching fraction of Zn^{2+} or SO_4^{2-}, K_d is the reaction rate constant (min^{-1}) for the chemical reaction between fluid reactant and solid particle at the surface of the solid particle, b is the stoichiometric coefficient of solid particle, C_A is the leaching solvent concentration ($mol.dm^{-3}$), ρ_B is the solid reactant molar density ($mol.m^{-3}$), R_o is the solid particle radius (m), and D_e is the effective diffusivity of the leaching solvent in the product layer.

$$1 - (1 - X)^{1/3} = \frac{bK_sC_A}{P_BR_0}t = K_ct \quad (3)$$

where X is the leaching fraction of Zn^{2+} or SO_4^{2-}, K_c is the reaction rate constant (min^{-1}) for diffusion through the product layer, and K_s is the surface reaction rate constant (m min^{-1}) [18].

Table 3 below shows the kinetic parameters obtained from the experimental data for the leaching of Zn^{2+} and SO_4^{2-} from tire pyrolytic char using H_2O_2 solution as a solvent. From Table 3, it is evident that the rate-limiting step for the leaching of both Zn^{2+} and SO_4^{2-} by H_2O_2 solvent solution is diffusion through the product layer. The regression coefficients obtained for diffusion through the product layer were closer to 1 than those obtained for the chemical reaction between the fluid reactant with the solid at the surface of the solid particle in the case of Zn^{2+} and SO_4^{2-}. Figures 9 and 10 show the linear relationship between $1 - 3(1 - X)^{2/3} + 2(1 - X)$ $vs\ t$ for Zn^{2+} and SO_4^{2-}, respectively, for all the process variables studied in this kinetic study. The rate constants were obtained as the gradient of the plots in Figures 9 and 10 for Zn^{2+} and SO_4^{2-}, respectively. From Table 3, it can be concluded that the reaction rate constant K_d increased as the values of the process variables increased, excluding the solid/liquid ratio where the opposite took place.

Table 3. Kinetic parameters and constants for leaching of Zn^{2+} and SO_4^{2-} from pyrolytic char.

	Product layer diffusion				Surface chemical reaction			
	Zn^{2+}		SO_4^{2-}		Zn^{2+}		SO_4^{2-}	
Process Variables	K_d (min^{-1})	R^2	K_d (min^{-1})	R^2	K_c (min^{-1})	R^2	K_c (min^{-1})	R^2
Stirring Speed (rpm)								
50	0.0015	0.8966	0.0009	0.9234	0.0027	0.8709	0.0021	0.8731
100	0.0037	0.9365	0.0013	0.9321	0.0044	0.9052	0.0025	0.8766
150	0.0048	0.9354	0.002	0.9231	0.0052	0.8838	0.0031	0.8706
200	0.007	0.9077	0.0023	0.9539	0.0068	0.87	0.0034	0.8948
Solvent Concentration (M)								
0.5	0.0021	0.6639	0.001	0.9597	0.0034	0.7693	0.0022	0.9052
1	0.0042	0.7682	0.0013	0.9382	0.0049	0.7572	0.0025	0.8746
1.5	0.0048	0.8775	0.0019	0.9242	0.0052	0.8359	0.003	0.8647
2	0.0085	0.8903	0.0026	0.9467	0.0078	0.8585	0.0036	0.8921
Temperature (°C)								
30	0.001	0.9416	0.0017	0.9824	0.0021	0.9087	0.0028	0.9312
45	0.0024	0.9733	0.0031	0.9701	0.0037	0.9511	0.004	0.935
60	0.0033	0.9692	0.001	0.962	0.0041	0.9442	0.0021	0.9275
75	0.0055	0.9772	0.0014	0.9675	0.0057	0.9584	0.0026	0.9266
Solid to liquid ratio (g/100 ml)								
0.5	0.004	0.8287	0.0025	0.9315	0.0047	0.8142	0.0035	0.8698
1	0.0077	0.887	0.0029	0.8919	0.0073	0.8475	0.0039	0.8404
1.5	0.0076	0.7771	0.0018	0.9136	0.0034	0.8028	0.0029	0.8613
2	0.0004	0.8365	0.0009	0.9059	0.0013	0.8181	0.002	0.8611

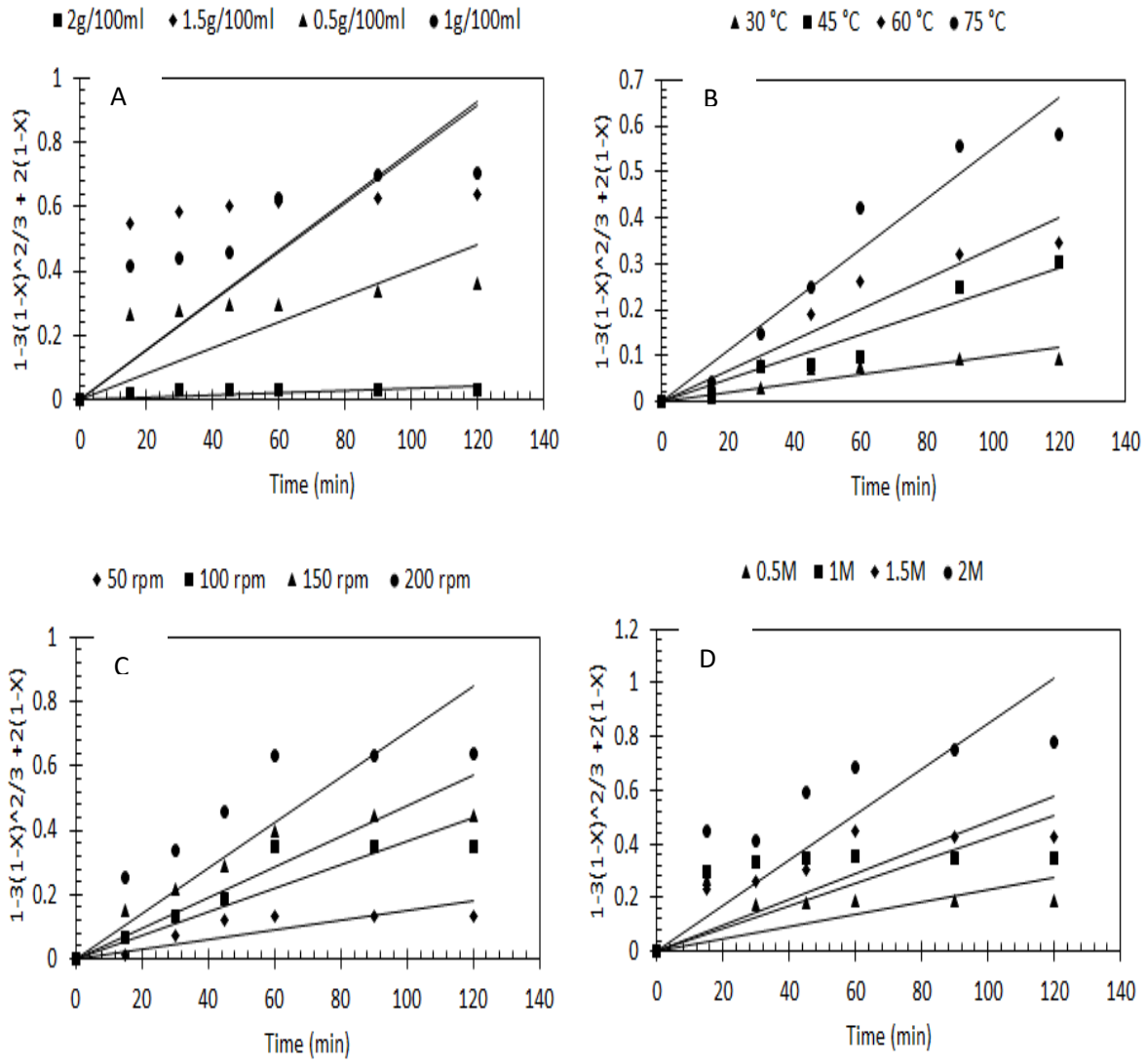

Figure 9. Linear relationship showing the difference of $1-3(1-X)^{2/3}+2(1-X)$ with reaction time for different (A) solid-to-liquid ratios, temperatures (B) stirring speeds (C), and solvent concentrations (D) for the leaching of Zn^{2+}.

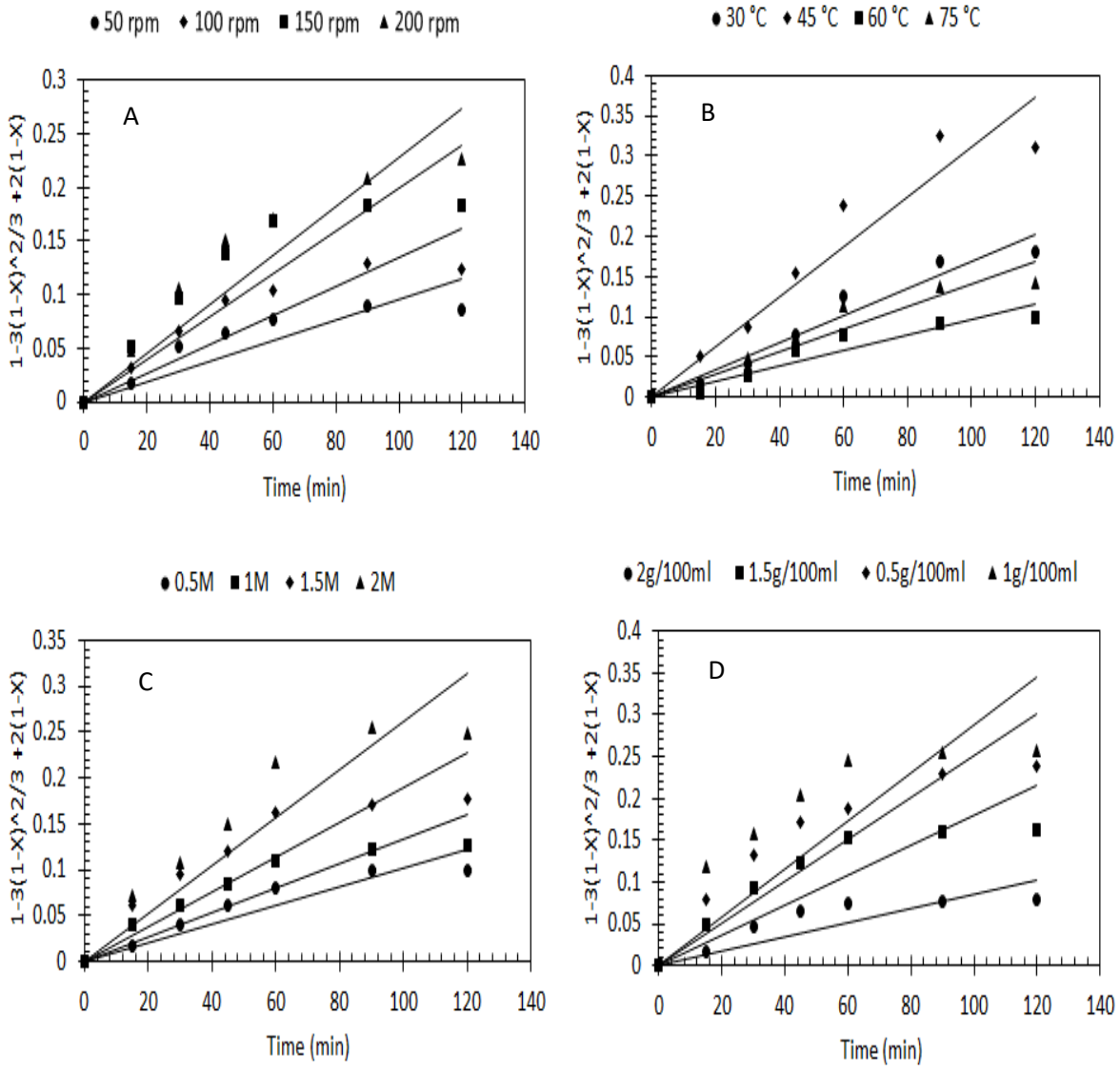

Figure 10. Linear relationship showing the difference of $1-3(1-X)^{2/3}+2(1-X)$ with reaction time for different stirring speeds(A), temperatures (B), concentrations (C), and solid-to-liquid ratios (D) for the leaching of SO_4^{2-}.

3.4. Activation energy

In heterogeneous reactions, it is crucial to determine the activation energy for the leaching process. It has been reported that high activation energy values greater than 40 kJ/mol suggest that the leaching process is controlled by chemical reaction, while activation energy values between 8 to 21 kJ/mol suggest the product layer diffusion as the rate-controlling step [28]. In cases where the activation energy may be between 25–43 kJ/mol, the process can be controlled by both diffusions through the product layer and chemical reaction [29,30]. The activation energy can be determined by plotting a plot of -ln(K_d) versus I/T, which originates from the following Arrhenius equation [26,27]:

$$k = k_0 e^{-\frac{E_a}{RT}} \quad (4)$$

Where k is the rate constant, k_0 is the frequency factor, E_a is the apparent activation energy, R is the universal gas constant ($J.mol^{-1}.K^{-1}$), and T is the temperature of the process (K). Figure 11 (A) and (B) display the Arrhenius plot for the leaching of Zn^{2+} and SO_4^{2-}. Applying the Arrhenius equation, the apparent activation energy values for the leaching of Zn^{2+} and SO_4^{2-} were calculated to be 36 $kJ.mol^{-1}$ and -11 $kJ.mol^{-1}$, respectively. The results suggest that the leaching of Zn^{2+} is controlled by a combination of product layer diffusion and chemical reaction. In contrast, the leaching of SO_4^{2-} is controlled by diffusion through the product layer [29,30]. Values of the frequency factor for the leaching of Zn^{2+} and SO_4^{2-} were obtained as the Y-intercept in Figure 11 as 724.95 and $3.4e^{-05}$, respectively.

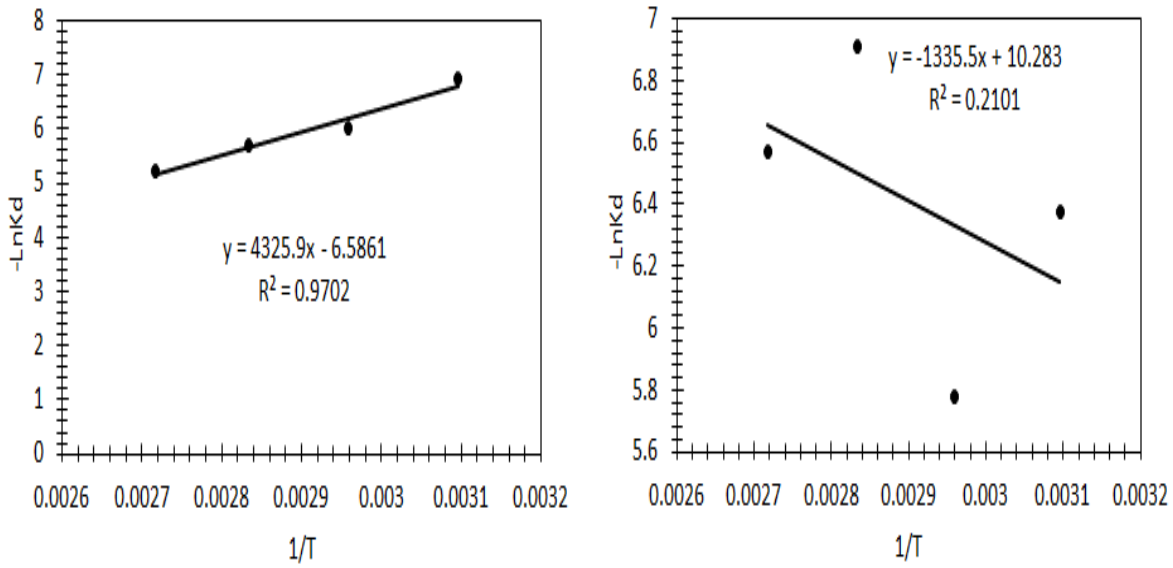

Figure 11. Arrhenius plot for the leaching of Zn^{2+} ions (A) and SO_4^{2-} ions (B).

3.5.Semi-empirical model

A semi-empirical model is an essential tool for correlating the experimental data for the leaching process [26]. It determines the effects of the process variables influencing the leaching process. The variables studied in this work include stirring speed, solvent concentration, temperature, and the solid-to-liquid ratio [25]. The following expression can represent a semi-empirical model:

$$K_d = K_o N^a C^b \left(\frac{S}{L}\right)^c e^{(-E_a/RT)} t \quad (5)$$

Combining Eqs. (2) and (5) establish the following relation:

$$1 - 3(1-X)^{2/3} + 2(1-X) = K_o N^a C^b \left(\frac{S}{L}\right)^c e^{(-E_a/RT)} t \quad (6)$$

N, C, and (S/L) represent the stirring speed, solvent concentration, and solid-to-liquid ratio. K_o is the frequency factor obtained from the Arrhenius Plot, and the constants *a*, *b*, and c represent the reaction orders. The reaction order *a*, for stirring Speed (N), was obtained from the gradient of the plot of $\ln k_d$ versus lnN. Values of the reaction orders *b* and *c* were obtained similarly through the gradients of the plots of $\ln k_d$ versus lnC and $\ln k_d$ versus ln(S/L), respectively. Figures 12 and 13 show the variation of

-lnk_d with -lnN, -lnC, and ln(S/L) for the leaching of Zn^{2+} and SO_4^{2-}, respectively. The values of the reaction orders for stirring Speed (N), solvent concentration (C), and solid-to-liquid ratio were obtained to be 0.9103, 1.0187, and 0.3654, respectively, for the leaching of Zn^{2+}. The values of the reaction orders for stirring speed (N), solvent concentration (C), and solid-to-liquid ratio were obtained to be 1.3935, 1.3872, and 1.1479, respectively, for the leaching of SO_4^{2-}.

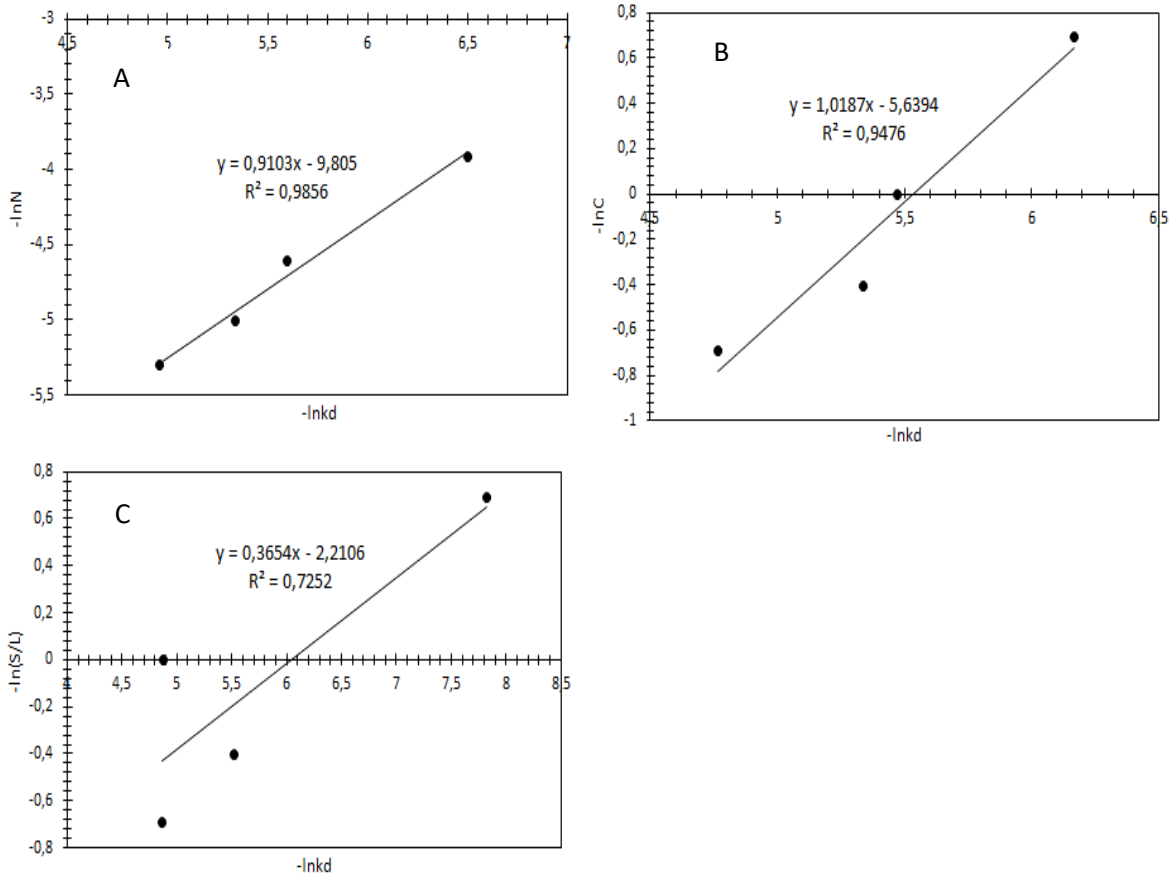

Figure 12. Variation of -lnK_d with -lnN (A), -lnC (B), and ln(S/L) (C) for the leaching of Zn^{2+}.

The values for the frequency factor were obtained from the Arrhenius Plot as 724.95 and $3.4e^{-5}$, respectively, for the leaching of Zn^{2+} and SO_4^{2-}. By substituting all the leaching variables into Eq.5, the semi-empirical models represented in Eqs. 7 and 8 were obtained, which can be used to represent the leaching of Zn^{2+} and SO_4^{2-} from tire pyrolytic char using an H_2O_2 solvent.

$$1 - 3(1 - X)^{2/3} + 2(1 - X) = 203.24N^{0.9103}C^{1.0187}\left(\frac{S}{L}\right)^{0.3654} e^{(-36000/RT)}t \quad (7)$$

$$1 - 3(1 - X)^{2/3} + 2(1 - X) = 5e^{-5}N^{1.3935}C^{1.3872}\left(\frac{S}{L}\right)^{1.1479} e^{(11000/RT)}t \quad (8)$$

4. Conclusions

We present the study of the leaching behavior of Zn^{2+} and SO_4^{2-} from tire pyrolytic char (TPO) using a solution of H_2O_2 as a solvent. We aimed to characterize the pyrolytic tire char before and after leaching and compare the samples. The results obtained from different characterization techniques,

including FTIR, SEM-EDS, and XRD, show that leaching of the tire pyrolytic char using H_2O_2 significantly affected the char's characteristics. Leaching studies were done to determine the effect of various process variables on the leaching rate of Zn^{2+} and SO_4^{2-}. The results showed that the process variables significantly affected Zn^{2+} and SO_4^{2-}leaching rates. The highest leaching percentages for Zn^{2+} and SO_4^{2-} were 96 % and 79 %, respectively. Using the experimental data, the shrinking core model showed that product layer diffusion was the rate-limiting step for both the leaching of Zn^{2+} and SO_4^{2-}. The apparent activation energies obtained for the leaching of Zn^{2+} show that the process is controlled by a combination of product layer diffusion and chemical reaction. For the leaching of SO_4^{2-}, the activation energy obtained confirmed that the rate-limiting step followed product layer diffusion. Semi-empirical models for the leaching of Zn^{2+} and SO_4^{2-} were developed to describe the leaching processes.

Use of AI tool declaration

The authors declare they have not used Artificial Intelligence (AI) tools in the creation of this article.

Acknowledgements

The authors would like to thank the Vaal University of Technology, Department of Chemical and Metallurgical Engineering for the VUT-COCA (Chemicals Consulting (Pty) Ltd) partnership, benefiting the DTI-THRIP (Technology and Human Resources for Industry Program) financial support.

Conflict of interest

The authors declare that there is no conflict of interest.

References

1. Sebola MR, Mativeng PT, Pretorius J (2018) A Benchmark Study of Waste Tyre Recycling in South Africa to European Union Practice. *Procedia CIRP, 25th CIRP Life Cycle Engineering (LCE) Conference*: 69: 950–955. https://doi.org/10.1016/j.procir.2017.11.137
2. Bockstal L, Berchem T, Schmetz Q, Richel A, et al. (2019) Devulcanization and reclaiming of tyres and rubber by physical and chemical processes: A review. *J Clean Prod* 236: 117574. https://doi.org/10.1016/j.jclepro.2019.07.049
3. Siddika A, Mamun MAA, Alyousef R, et al. (2019) Properties and utilizations of waste tyre rubber in concrete: A review. *Constr Build Mater* 224: 711–731. https://doi.org/10.1016/j.conbuildmat.2019.07.108
4. Sattayanurak S, Sahakaro K, Kaewsakul W, et al. (2019) Utilization of Organoclay as Secondary Filler in Silica-reinforced Natural Rubber Tyre Tread Compounds. In: *Fall 196th Technical Meeting of Rubber Division* In press.
5. Shulman VL (2019) Chapter 26 Tyre Recycling, In: Letcher TM, Vallero DA (Eds.), Waste, 2Eds., Academic Press, 489–515. https://doi.org/10.1016/B978-0-12-815060-3.00026-8
6. Ramarad S, Khalid M, Ratnam CT, et al. (2015) Waste tyre rubber in polymer blends: A review on the evolution, properties and future. *Prog Mater Sci* 72:100–140. https://doi.org/10.1016/j.pmatsci.2015.02.004

7. Antoniou N, Zabaniotou A (2015) Experimental proof of concept for a sustainable End of Life Tyres pyrolysis with energy and porous materials production. *J Clean Prod* 101: 323–336. https://doi.org/10.1016/j.jclepro.2015.03.101
8. Choi G-G, Jung S-H, Oh S-J, et al. (2014) Total utilization of waste tyre rubber through pyrolysis to obtain oils and CO2 activation of pyrolysis char. *Fuel Process Technol* 123: 57–64. https://doi.org/10.1016/j.fuproc.2014.02.007
9. Hürdoğan E, Ozalp C, Kara O, et al. (2017) Experimental investigation on performance and emission characteristics of waste tyre pyrolysis oil–diesel blends in a diesel engine. *Int J Hydrog Energy* 42:23373–23378. https://doi.org/10.1016/j.ijhydene.2016.12.126
10. Martínez JD, Puy N, Murillo R, et al. (2013) Waste tyre pyrolysis–A review. *Renew Sustain Energy Rev* 23:179–213. https://doi.org/10.1016/j.rser.2013.02.038
11. Martínez JD, Cardona-Uribe N, Murillo R, et al. (2019) Carbon black recovery from waste tyre pyrolysis by demineralization: Production and application in rubber compounding. *Waste Manag* 85: 574–584. https://doi.org/10.1016/j.wasman.2019.01.016
12. Chen D, Ling C, Wang T, et al. (2018) Prediction of tyre-pavement noise of porous asphalt mixture based on mixture surface texture level and distributions. *Constr Build Mater* 173: 801–810. https://doi.org/10.1016/j.conbuildmat.2018.04.062
13. Bocca B, Forte G, Petrucci F, et al. (2009) Metals contained and leached from rubber granulates used in synthetic turf areas. *Sci Total Environ* 407: 2183–2190. https://doi:10.1016/j.scitotenv.2008.12.026
14. Yamaguchi K, Kinoshita T, Akita S (2006) Thermal treatment of waste tyre fly ash with polyvinyl chloride: Selective leaching of Zinc with water. *Ind Eng Chem Res* 45: 1211–1216. https://doi.org/10.1021/ie051118x
15. Zou C, Ren Y, Li S, et al. (2022) Effects of molten salt thermal treatment on the properties improvement of waste tyre pyrolytic char. *Waste Manag* 149: 53–59. https://doi.org/10.1016/j.wasman.2022.05.028
16. Jiang G, Pan J, Deng W, et al. (2022) Recovery of high pure pyrolytic carbon black from waste tyres by dual acid treatment. *J Clean Product* 374: 133893. https://doi.org/10.1016/j.jclepro.2022.133893
17. Bernardo M, Lapa N, Gonçalves M, et al. (2012) Study of the organic extraction and acidic leaching of chars obtained in the pyrolysis of plastics, tyre rubber and forestry biomass wastes. *Proced Eng* 42: 1739–1746. https://doi.org/10.1016/j.proeng.2012.07.567
18. Levenspiel O (1972) Chemical Reaction Engineering, In: John Wiley and Sons, 3Eds., New York: 578.
19. Dube G, Osifo P, Rutto H (2014) Preparation of bagasse ash/CaO/ammonium acetate sorbent and modelling their desulphurization reaction. *Clean Techn Environ Policy* 16: 891–900. https://doi.org/10.1007/s10098-013-0681-8
20. Rutto H, Enweremad C (2012) Dissolution of a South African calcium based material using urea: An optimized process. *Korean J Chem Eng* 29: 1–8. https://doi.org/10.1007/s11814-011-0136-z
21. He F, Ma B, Wang C, Zuo Y, et al. (2022) Dissolution behavior and porous kinetics of limonitic laterite during nitric acid atmospheric leaching. *Minerals Eng* 185: 107671. https://doi.org/10.1016/j.mineng.2022.107671
22. Ajiboye EA, Panda PK, Adebayo AO, et al. (2019) Leaching kinetics of Cu, Ni and Zn from waste silica rich integrated circuits using mild nitric acid. *Hydrometallurgy* 188: 161–168. https://doi.org/10.1016/j.hydromet.2019.06.016

23. Seng-eiad S, Jitkarnka S (2016) Untreated and HNO_3-treated pyrolysis char as catalysts for pyrolysis of waste tyre: In-depth analysis of tyre-derived products and char characterization. *J Anal Appl Pyrolysis* 122: 151–159. https://doi.org/10.1016/j.jaap.2016.10.004
24. Manoj B (2012) Chemical demineralization of high volatile Indian bituminous coal by carboxylic acid and characterization of the products by SEM/EDS. *J Environ Res Dev* 6: 653–659. http://archives.christuniversity.in/items/show/880
25. Zhou J, Zhao J, Yang F, et al. (2020) Leaching kinetics of potassium and aluminum from phosphorus-potassium associated ore in HCl-CaF2 system. *Sep Purif Technol* 253: 117528. https://doi.org/10.1016/j.seppur.2020.117528
26. Koech L, Everson R, Neomagus H, et al. (2015) Leaching kinetics of bottom ash waste as a source of calcium ions. *J Air Waste Manag Assoc* 65: 126–132. https://doi.org/10.1080/10962247.2014.978958
27. Koech L, Rutto H, Everson R, et al. (2014) Semi-empirical model for limestone dissolution in adipic acid for wet flue gas desulfurization. *Chem Eng Technol* 37: 1919–1928. https://doi.org/10.1002/ceat.201400248
28. Raza N, Zafar ZI, Najam-ul-Haq (2013) An analytical model approach for the dissolution kinetics of magnesite ore using ascorbic acid as leaching agent. *Int J Met* 1: 352496. https://doi.org/10.1155/2013/352496
29. Cao R, Jia Z, Zhang Z, et al. (2020) Leaching kinetics and reactivity evaluation of ferronickel slag in alkaline conditions. *Cem Concr Res* 137: 106202. https://doi.org/10.1016/j.cemconres.2020.106202
30. Sharma S, Agarwal GK, Dutta NN (2020) Kinetic study on leaching of Zn and Cu from spent low-temperature shift catalyst ($CuO/ZnO/Al_2O_3$): application of taguchi design. *J Mater Cycles Waste Manag* 22: 1509–1520. https://doi.org/10.1007/s10163-020-01038-x
31. He J, Yang J, Tariq SM, et al (2020) Comparative investigation on copper leaching efficiency from waste mobile phones using various types of ionic liquids. *J Clean Product* 256: 120368. https://doi.org/10.1016/j.jclepro.2020.120368
32. Rozmysłowska-Wojciechowska A, Mitrzak J, Szuplewska A, et al. (2020) Engineering of 2D Ti3C2 MXene surface charge and its influence on biological properties. *Materials* 10: 2347. https://doi.org/10.3390/ma13102347
33. Kumar A, Choudhary R, Kumar A (2021) Aging characteristics of asphalt binders modified with waste tire and plastic pyrolytic chars. *PLoS One* 19: 16. https://doi.org/10.1371/journal.pone.0256030
34. Czarna-Juszkiewicz D, Kunecki P, Cader J, et al. (2023) Review in waste tire management—potential applications in mitigating environmental pollution. *Materials* 16: 5771. https://doi.org/10.3390/ma16175771
35. Li S, Tran TQ, Li Q, et al. (2023) Zn leaching recovery and mechanisms from end-of-life tire rubber. *Resour Conserv Recycl* 194: 107004. https://doi.org/10.1016/j.resconrec.2023.107004
36. Undri A, Sacchi B, Cantisani E, et al. (2013) Carbon from microwave assisted pyrolysis of waste tires. *J Anal Appl Pyrol* 104: 396–404. https://doi.org/10.1016/j.jaap.2013.06.006
37. Battsengel A, Batnasan A, Narankhuu A, et al. (2018) Recovery of light and heavy rare earth elements from apatite ore using sulphuric acid leaching, solvent extraction and precipitation. *Hydrometallurgy* 179: 100–109. https://doi:10.1016/j.hydromet.2018.05.024

38. Faraji F, Alizadeh A, Rashchi F, et al. (2022) Kinetics of leaching: A review. *Rev Chem Eng* 38: 113–148. https://doi.org/10.1515/revce-2019-0073

AIMS Press